Bacterial predation transforms the landscape and community assembly of biofilms

Highlights

- Biofilms with high cell packing are protected from bacterial predator access
- The protection effect strongly alters biofilm microlandscapes after predation
- Predation on the periphery of biofilms loosens their local architecture
- These changes in biofilm structure allow other bacteria to invade prey biofilms

Authors

Benjamin R. Wucher, Mennat Elsayed, James S. Adelman, Daniel E. Kadouri, Carey D. Nadell

Correspondence

carey.d.nadell@dartmouth.edu

In brief

Wucher et al. show that biofilms of the pathogen *Vibrio cholerae*, a susceptible prey target to the predator *B. bacteriovorus*, can protect themselves from predator attack if they reach a critical cell-cell packing threshold. This protection threshold results in dramatic alterations of microscopic biofilm landscape structure and community assembly.





Report

Bacterial predation transforms the landscape and community assembly of biofilms

Benjamin R. Wucher, Mennat Elsayed, James S. Adelman, Daniel E. Kadouri, and Carey D. Nadell1,4,*

- ¹Department of Biological Sciences, Dartmouth College, 78 College Street, Hanover, NH 03755, USA
- ²Department of Oral Biology, Rutgers School of Dental Medicine, 110 Bergen Street, Newark, NJ 07101, USA
- ³Department of Biological Sciences, The University of Memphis, 3700 Walker Avenue, Memphis, TN 38117, USA

*Correspondence: carey.d.nadell@dartmouth.edu https://doi.org/10.1016/j.cub.2021.03.036

SUMMARY

The bacterium *Bdellovibrio bacteriovorus* attaches to the exterior of a Gram-negative prey cell, enters the periplasm, and harvests resources to replicate before lysing the host to find new prey.¹⁻⁷ Predatory bacteria such as this are common in many natural environments, ⁸⁻¹³ as are groups of matrix-bound prey cell clusters, termed biofilms.¹⁴⁻¹⁶ Despite the ubiquity of both predatory bacteria and biofilm-dwelling prey, the interaction between *B. bacteriovorus* and prey inside biofilms has received little attention and has not yet been studied at the micrometer scale. Filling this knowledge gap is critical to understanding bacterial predator-prey interaction in nature. Here we show that *B. bacteriovorus* is able to attack biofilms of the pathogen *Vibrio cholerae*, but only up until a critical maturation threshold past which the prey biofilms are protected from their predators. Using high-resolution microscopy and detailed spatial analysis, we determine the relative contributions of matrix secretion and cell-cell packing of the prey biofilm toward this protection mechanism. Our results demonstrate that *B. bacteriovorus* predation in the context of this protection threshold fundamentally transforms the sub-millimeter-scale landscape of biofilm growth, as well as the process of community assembly as new potential biofilm residents enter the system. We conclude that bacterial predation can be a key factor influencing the spatial community ecology of microbial biofilms.

RESULTS AND DISCUSSION

Biofilm formation is a common mode of microbial life in which cells of one or more species produce surface-attached or free-floating communities that are bound by a self-produced polymer matrix. ^{14–16} Biofilms are fundamental to microbial ecology in contexts including marine snow, ^{17–22} the rhizosphere, ²³ microbiomes on or within multicellular organisms, ^{24,25} and acute and chronic infections. ^{26–28} Bacteria dwelling in these communities collectively determine their architecture using many mechanisms, including the matrix; this architecture then influences surface occupation, dispersal, competition for space and nutrients, and protection from exogenous threats. ^{29–33}

Many studies have shed light on the mechanisms that biofilm-dwelling bacteria use in response to bottom-up selective pressures such as spatial or nutritional competition. 16,22,31,34-45 Others have examined the influence of top-down selective pressures, such as toxin exposure and predation, which can have profound impacts on the behavior and survival of biofilm communities. For example, the effects of antibiotics on biofilms have been investigated in detail; some but not all antimicrobials are blocked from diffusing completely into biofilms, and those that do permeate biofilms can substantially alter their spatial organization. Other recent work has assessed the interaction of bacteriophages and biofilms at single-cell resolution, finding that some biofilms can block phage entry using

components of the secreted matrix. 32,52-55 The micrometer-scale dynamics of interaction between biofilms and larger predatory threats have received less attention, however. A key example of such a predator is *Bdellovibrio bacteriovorus*, which is ubiquitous in natural environments. 56-60

B. bacteriovorus, a delta-proteobacterium approximately 1 μm in length, most often exhibits an obligate predatory lifestyle in which it targets Gram-negative prey, bores through the outer membrane into the periplasm, harvests resources to replicate, and lyses the host cell in search of new prey. ^{1–7} *B. bacteriovorus* can predate *Escherichia coli* and *Pseudomonas fluorescens* within biofilms in static culture and under flow, ⁶¹ and numerous studies have isolated *B. bacteriovorus* directly from biofilms on abiotic substrata and the surfaces of animals and plants in aquatic environments. ^{8–13} Predatory bacteria and biofilm communities are thus widespread in nature and commonly interact, ^{4,57,62–64} but the detailed spatial ecology of *B. bacterivorous* predation in this context is not well understood.

In aquatic environments, predatory bacteria are population modulators of the *Vibrio* clade, ⁶⁴ and *V. cholerae* is a known susceptible prey target of *B. bacterivorous*. ⁶⁵ We therefore chose *V. cholerae*, whose architectural dynamics and matrix components have been characterized in depth, ^{15,29,30,66–70} as a model organism to examine *B. bacteriovorus* interaction with prey biofilms. Using a combination of microfluidic culture, confocal imaging, and detailed spatial analysis, we explore how bacterial

⁴Lead contact



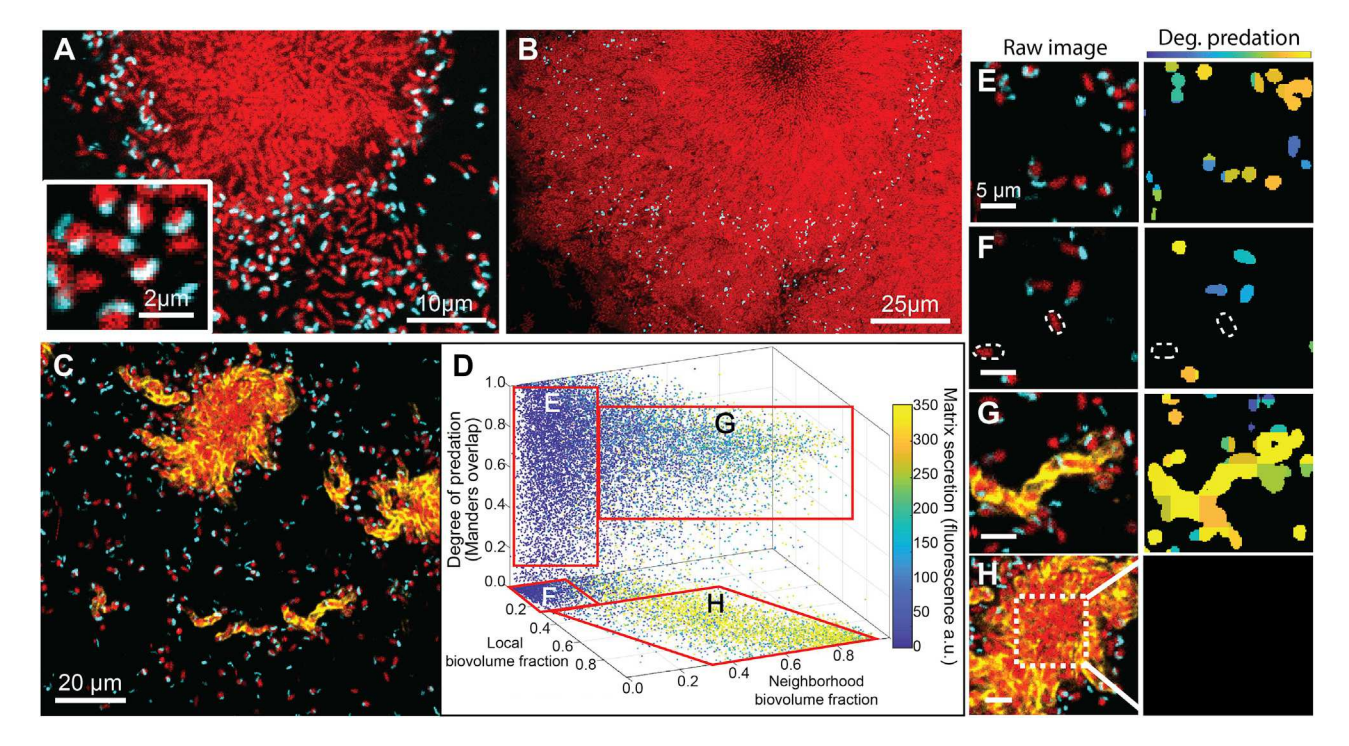


Figure 1. B. bacteriovorus predation of V. cholerae biofilms and its relationship to prey biofilm matrix production and cell packing Prey biofilms (red) were grown for 48 h prior to exposure to predator cells (cyan).

- (A) Thirty minutes after introduction, predator cells have preyed upon singleton cells, forming bdelloplasts (inset). Predator cells also appear able to access prey on the periphery, but not within the innermost regions, of V. cholerae biofilm clusters.
- (B) Forty-eight hours after introduction, V. cholerae biofilm clusters showed net positive growth, trapping B. bacteriovorus in the expanding front.
- (C) Raw fluorescence image showing a horizontal cross section of a matrix-labeled biofilm (the matrix protein RbmA is now labeled in yellow).
- (D) Image analysis of biofilms exposed to predatory bacteria after 2 h. The x and y axes denote neighborhood and local biovolume fractions, respectively. The z axis denotes the degree of predation. Any points above the bottom x-y plane denote prey cells in the process of being killed by predatory bacteria. Data points are color-coded according to local matrix fluorescence intensity (n = 23).
- (E-H) Raw images and corresponding heatmaps for degree of predation. In the raw images at left, prey cells are red, predators are cyan, and matrix is yellow. In the heatmaps at right, blue/teal indicates a predator cell attached to a prey cell, and orange/yellow indicates a predator cell inside a prey cell.
- (E and F) Isolated singleton cells are fully exposed and tend to be killed off by B. bacteriovorus (E), though some singleton cells have not yet been found by a predator, highlighted by the dotted outlines in (F).
- (G) Small biofilm clusters producing extracellular matrix are nevertheless fully susceptible to predation.
- (H) Though the periphery regions of large biofilm clusters are still susceptible to predation—as in (G)—the internal regions of these clusters with high cell-packing are protected.

See also Figure S1.

predation pressure influences biofilm structure and composition. We find that exposure to bacterial predators fundamentally alters the landscape of biofilm growth and communal defense against infiltration by newly arriving planktonic bacteria.

V. cholerae biofilms have a maturation threshold for protection from B. bacterivorous

To evaluate the interaction between pre-formed resident V. cholerae biofilms and their bacterial predators, we first cultivated V. cholerae on glass surfaces in microfluidic flow devices. Approximately 48 h after the initial surface inoculation and initiation of flow, we introduced B. bacteriovorus into the chambers over a period of 30 min, followed by resumption of predatorfree medium flow for the remainder of the experiment. Biofilms were then imaged through their entire 3D volume by confocal microscopy (STAR Methods).

Successful predation could be seen throughout the microfluidic arena among singleton prey V. cholerae. Cells on the periphery of biofilm clusters appeared susceptible as well, but the centers of larger biofilm clusters were devoid of predator cells (Figure 1A). Images taken 48 h after initial predator exposure showed that prey cells on the interior of these clusters remained unexposed to predation; remaining B. bacteriovorus cells were immobilized in the matrix milieu around resident prey throughout the expanding biofilm front (Figure 1B). These results suggest that one or more features of V. cholerae biofilm architecture inhibit predator cells from entering the biofilm interior.

We next sought to understand how V. cholerae biofilm structure influences spatial access by predator cells. Prior work has linked the biofilm matrix to protection of biofilms from entry by bacteriophages and competing microbes; 32,37,52 following this precedent, we were curious as to the contribution of the matrix in protection from B. bacteriovorus predation. To pursue this question, we introduced a 3x-FLAG epitope to the N terminus of the V. cholerae matrix protein RbmA; this construct allowed

Current Biology Report



us to directly visualize the matrix without altering its function. ^{37,66,67} RbmA has been extensively characterized as a key matrix component, along with vibrio polysaccharide (VPS), in controlling cell-cell packing and alignment architecture within biofilms of this species. ^{29,30,66,68} Our visualizations showed that *B. bacterivorous* localized within the outermost layers of cells and matrix material in the periphery of larger biofilm clusters. *V. cholerae* cells outside of the matrix were frequently preyed upon (Figures 1C and S1A). Visual inspection alone, however, could not determine whether proximity to matrix was sufficient on its own to protect prey from predatory bacteria.

To resolve this uncertainty, we performed a high-resolution analysis of the amount of secreted matrix, the cell-cell packing among prey V. cholerae cells, and the relationship between these biofilm features and local predation by B. bacteriovorus. We separated predator and prey biovolumes from background by segmentation and dissected them into a 3D grid, with each cubic grid unit measuring 2.6 µm on a side (Figure S1B). At this resolution, the grid units could contain \sim 3–5 cells of *V. cholerae* and/or B bacteriovorus. For each segmented V. cholerae biovolume, we calculated (1) the local accumulation of RbmA matrix, (2) the local biovolume fraction (i.e., how much of a 1.5 µm shell around each segmented V. cholerae was occupied by other V. cholerae), (3) the neighborhood biovolume fraction (i.e., how much of a 6 µm shell around each segmented V. cholerae was occupied by other V. cholerae), and finally (4) an overlap coefficient between V. cholerae and B. bacteriovorus (i.e., the degree of predation; STAR Methods; Figures S1B-S1F). Note that the local and neighborhood biovolume fractions are both proxies for cell-cell packing of prey V. cholerae, but on two spatial scales, so they yield different information about localized versus more distal cellpacking architecture.

Using the metrics described above, we analyzed n = 23 independent image stacks, which revealed four different sub-populations (Figure 1D). We label these E-H to correspond with examples of each in Figures 1E-1H. Population E includes singleton V. cholerae cells with zero matrix and low local and neighborhood biovolume fractions, and which have been preyed upon by B. bacteriovorus (Figure 1E). Population F includes singletons much like population E, but which have not yet been found by a predator cell (Figure 1F). Population G includes V. cholerae clusters that have begun producing matrix, but which have not yet formed hemi-spherical groups; this sub-population has detectable matrix signal, high local biovolume fraction, but low neighborhood biovolume fraction (Figure 1G). Also in group G are units on the outer periphery of larger biofilm clusters. The cells in group G, despite accumulating matrix and high local density, are highly susceptible to predation (Figure S1G). Lastly, population H includes groups of cells on the interior of larger biofilm clusters; these have high matrix accumulation, high local and neighborhood biovolume fractions, and almost complete protection from predation (Figure 1H). Overall, these results suggest that local matrix accumulation alone is not sufficient for protection from B. bacteriovorus; rather, a combination of matrix secretion and cell-cell packing is at play.

To further explore the interaction between matrix production, cell-cell packing, and predation protection, we studied two additional mutants and their susceptibility to $B.\ bacteriovorus.$ One is a vpv^{W240R} point mutant that constitutively produces

extracellular matrix—we refer to this strain as a matrix hypersecretor. The other, $\Delta rbmA$, harbors a clean deletion of the rbmA locus and cannot produce the core matrix protein RbmA. The hyper-secretor rapidly generates highly compact biofilm clusters relative to wild type (WT), $^{71-73}$ and the $\Delta rbmA$ strain produces biofilms with far looser cell-cell packing and altered cell orientation architecture. 16,29,30,37,66,67 These strains—and WT for comparison—were grown in monoculture microfluidic devices and subjected to B. bacterivorous (Figures 2A–2C).

The resulting image data were again segmented and dissected into a cubic grid for spatial analysis as described above. Figures 2D-2F show heatmaps of local versus neighborhood biovolume fraction with points color-coded according to predation state; Figures 2G and 2H show analogous heatmaps, but with points color-coded according to local RbmA accumulation. From this analysis it is evident that both WT and matrix hyper-secreting strains have a critical neighborhood biovolume fraction (~0.8) above which patches of cells are largely protected from predator exposure (Figures 2D, 2E, S2A, and S2B). Logistic regression of predation probability as a function of our three biofilm architecture measurements confirmed that neighborhood biovolume fraction is the dominant factor influencing the likelihood that V. cholerae prey succumb to B. bacteriovorus predation (these analyses are developed in Tables S1 and S2). A larger proportion of clusters of the matrix hyper-secreting strain reached this threshold before predator exposure, and so this strain had greater overall protection against predation (Figures S2C-S2E); hyper-secretor clusters were still susceptible to predation along their periphery in the same manner as larger WT biofilm clusters (Figures S2F-S2I). Importantly, however, even though the matrix hyper-secreting strain has a higher signature of matrix secretion (Figures 2G and 2H), its threshold biovolume fraction for protection against B. bacteriovorus is the same as that of WT. By comparison, biofilms of the $\Delta rbmA$ strain never reach the biovolume fraction threshold required for protection against predator attack, and nearly all cells are killed (Figure 2F).

Altogether these data suggest that it is not the extracellular matrix by itself but rather the collective cell-cell packing that emerges from cell-matrix and cell-cell interaction that ultimately provides protection against spatial access by B. bacteriovorus. Another notable implication of our analysis is that there are two advancing fronts on the periphery of growing V. cholerae biofilms. The first is the true outer layer of biofilm expansion in which cells are producing extracellular matrix but have not yet achieved the cell-packing required for B. bacteriovorus protection. The second front, lagging behind the first, is that at which matrix and cell-packing have fully matured, conferring lasting protection against invasion by bacterial predators. Our results imply that the consolidation rate of this secondary front exceeds the rate of infiltration and predation by B. bacteriovorus on the biofilm periphery, allowing the biofilm to maintain positive net growth despite grazing by the predators.

B. bacterivorous predation transforms the landscape of **V.** cholerae biofilm growth

Our results thus far establish a critical cell-packing threshold above which biofilms of *V. cholerae* survive exposure to *B. bacteriovorus* (Figures 2D, 2E, and S2); though the predator



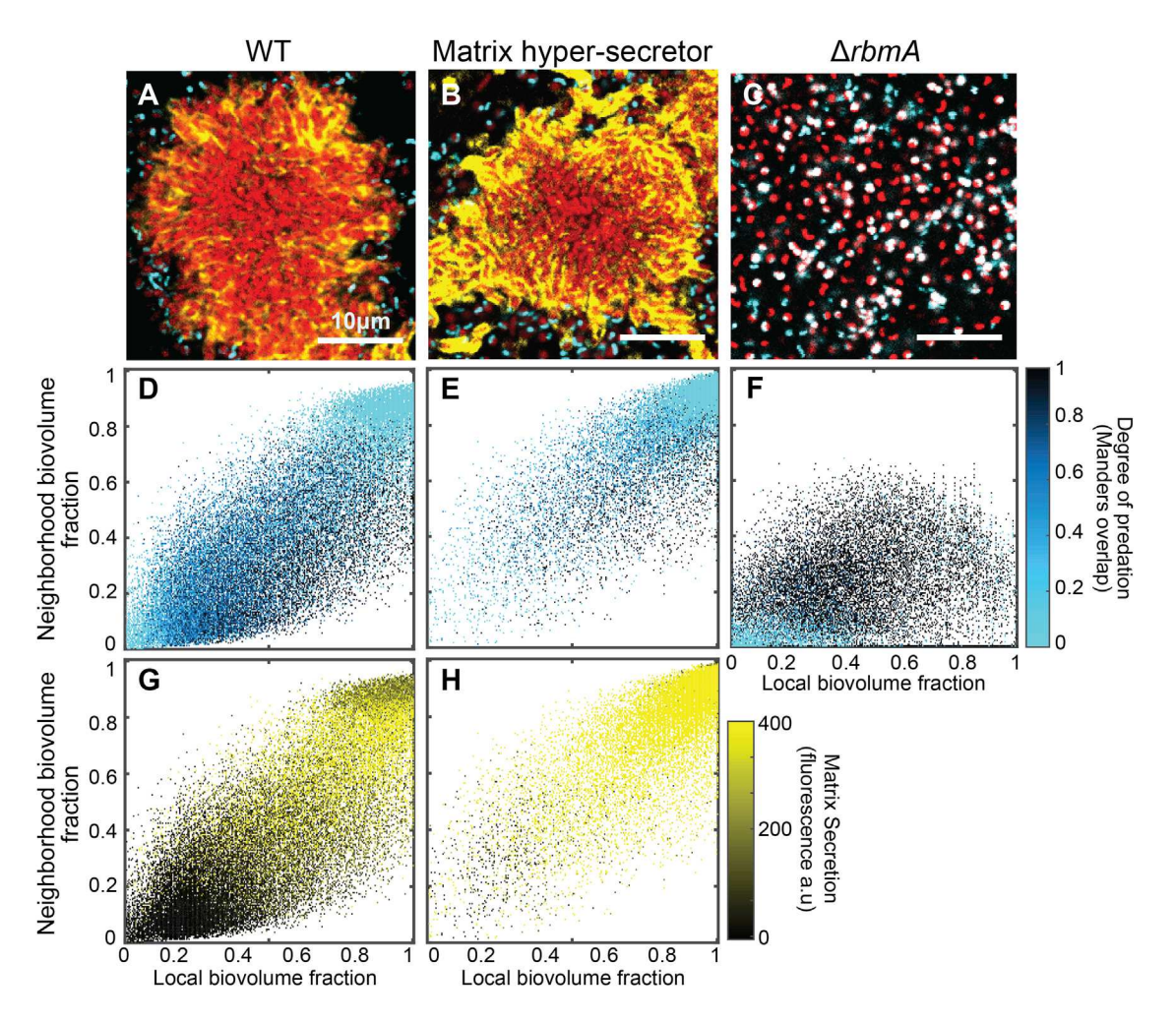


Figure 2. A critical threshold of neighborhood biovolume fraction correlates with prey cell protection from predation

(A–C) Images of V. cholerae biofilm clusters of WT, matrix hyper-secreting, and ΔrbmA strains 2 h after predator introduction. V. cholerae cells are shown in red, B. bacteriovorus is shown in cyan, and immunostained RbmA-FLAG matrix protein is shown in yellow. Biofilms were segmented and analyzed by dissecting the total system into a cubic grid as detailed in the main text. The segmented biovolumes in each grid unit were analyzed individually to produce the heatmaps described below.

(D-F) Heatmap plots for the degree of predation in biofilms of the three strains shown in (A)-(C), respectively (n = 6 for each strain). The horizontal axis denotes local biovolume fraction, and the vertical axis denotes neighborhood biovolume fraction. Light blue points correspond to biofilm volume units that are protected from predation, dark blue points denote areas with predation initiating at the cell exterior, and black points denote areas fully predated. Note the critical threshold neighborhood biovolume fraction of approximately 0.8 above which biofilms are protected from predation in (D) and (E).

(G and H) Heatmaps plots for RbmA matrix accumulation in biofilms of the two strains shown in (A) and (B), respectively (n = 6 for each strain). There is no entry for the $\Delta rbmA$ strain because it cannot produce the matrix protein being immunostained. Axes are as for (D)-(F). The black-to-yellow scaling relates the matrix accumulation for each point. Note in comparing (E) and (H) in particular that high matrix production by itself does not confer predator protection; rather, matrixreplete regions of the biofilm must first reach the critical neighborhood cell-packing threshold before predators are spatially excluded. See also Figure S2 and Tables S1 and S2.

can continue grazing on the periphery of these biofilms, the prey cell clusters maintain positive net growth. This observation reminded us of studies at much larger spatial scales in the context of forest ecology. Our findings are comparable to browsing and fire traps, which can limit the recruitment of tree saplings to adult trees: only saplings past a size threshold survive herbivore grazing and fire to become adults. 74,75 Depending on grazing and fire frequency, this effect can generate vastly different distributions of tree biomass on continental scales.⁷⁶ With this analogy in mind, we were curious as to how exposure to B. bacteriovorus influences the sub-millimeter-scale landscape of *V. cholerae* biofilms.

We explored this question by repeating the experiment above with a different imaging regime. V. cholerae was grown in microfluidic devices for 48 h before a single introduction of B. bacterivorous, followed by a return to predator-free media influx. In control treatments, the same tubing exchanges were performed, but no predators were introduced. We then imaged the biofilms by confocal microscopy 48 h later, which revealed dramatic differences between the two treatments. Control chambers contained a wide array of cell cluster sizes (Figure 3A). The frequency distribution of neighborhood biovolume fraction in this condition was broad with a shallow peak at \sim 0.35 (Figure 3C).

Current Biology Report



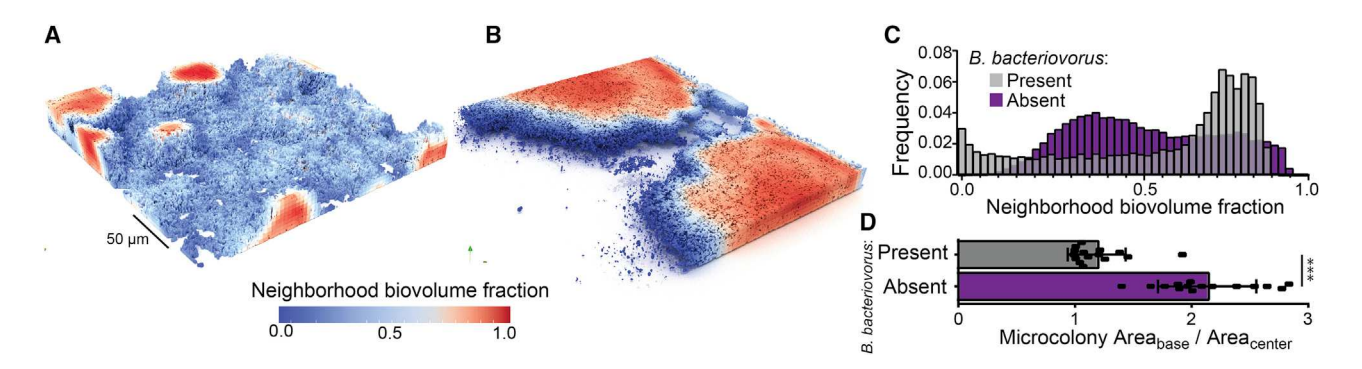


Figure 3. Exposure to predation by B. bacteriovorus shifts the microscopic landscape of prey biofilms

(A) In the absence of predatory bacteria, V. cholerae produces biofilms with abundant small clusters that have high internal neighbor volume fraction and low peripheral neighborhood volume fraction.

(B) Under predation by B. bacteriovorus, single cells and small colonies below a neighborhood cell-packing threshold are exposed and killed, leaving few remaining clusters, which are then free to grow very large.

(C) Frequency distributions of neighborhood volume fraction for biofilms exposed or unexposed to B. bacteriovorus predation. Biofilms exposed to predation show a strong shift toward high neighborhood volume fraction. These distributions were confirmed to be significantly different via a Kolmogorov-Smirnov test (p < 0.001. n = 15).

(D) Quantification of the average ratio of basal area to mid-plane area for biofilms with and without exposure to predators. Exposed biofilms, because they have room to grow into much larger columnar structures, have a ratio of ~1; unexposed biofilms, in which clusters compete more for space, remain hemispherical, such that they are larger at their base than they are at their mid-plane (***p < 0.001, Wilcoxon signed-rank test with n = 15). See also Figure S3.

Biofilms exposed to B. bacteriovorus were strongly shifted toward very large cell clusters that had reached the ceiling of the chambers and grown into columnar structures, in contrast to the hemispherical biofilm microcolonies observed in the control chambers (Figure 3B). We could test whether the difference in biofilm cluster shape between the two treatments was consistent across all replicates by measuring the ratio of biomass at the base of biofilm clusters to that at the chamber mid-plane. This ratio was \sim 2 in control chambers but transitioned to 1 in predator-exposed chambers, reflecting the change from hemispherical to columnar cell groups (Figure 3D). The distribution of neighborhood volume fraction for predatorexposed biofilms showed a pronounced shift toward high values in the range of 0.8, the critical cutoff identified above for protection from predator attack (Figure 3C). This shift occurred within the first 16 h after predator exposure (Figures S3A-S3C). In chambers with predators introduced, the space around large clusters was mostly unoccupied, presumably due to killing by B. bacteriovorus, which contrasted sharply with control chambers in which areas surrounding cell clusters were occupied by nascent biofilm clusters or cell monolayers (Figures S3D and S3E).

B. bacterivorous exposure alters biofilm surface structure and allows infiltration by newly arriving

An additional observation from our long-term imaging experiments was that among biofilm clusters that survive predator exposure, their outermost layers-which remained susceptible to B. bacteriovorus — look to be more loosely packed than those of biofilms in the control condition (Figure 3B). Cell packing in the exterior of biofilms is an important element of a community barrier function in V. cholerae and other microbes, which protects against intra- and inter-specific infiltration. 37,52 Typically, V. cholerae biofilms rarely allow for successful surface colonization by other bacteria, and they are extremely resistant to infiltration into their interior. 37,52 The packing architecture that confers this protection is a result of cell-matrix and cellcell interactions that altogether form the basis of structural strength in their biofilms. We hypothesized that by killing a fraction of cells in the biofilm exterior layer, B. bacteriovorus partially compromises this packing architecture, perhaps rendering them less resistant to entry by other bacteria including conspecific or heterospecific competitors. To test this idea, we once again grew V. cholerae biofilms for 48 h and subjected them to B. bacteriovorus. Forty-eight hours later, we introduced new competitors to the environment in the form of an isogenic V. cholerae strain that produced a different fluorescent protein than the resident biofilm, so the two could be distinguished from each other and the predator cells.

In control chambers without predator exposure, resident biofilms blocked invasion of newly introduced cells, as seen previously³⁷ (Figure 4A). In contrast, predator-exposed biofilms permitted substantial infiltration of competitors past their outer boundaries (Figures 4B-4D). Quantifying these results by image analysis, invasion of colonizing competitors into predatorexposed biofilms was ~40-fold greater than for control biofilms (Figure 4E). Areas of resident biofilms with many B. bacterivorous cells present also appeared to have a higher density of invading cells (Figures 4C and 4D). Analyzing these data at finer spatial resolution, we found a linear correlation between the number of invading cells present in a given location as a function of how much predation that location had experienced (Figure 4F). This outcome is consistent with our hypothesis that B. bacteriovorus predation disrupts local biofilm architecture and renders it more openly exposed to entry by other cells. Importantly, we could show that the same qualitative pattern applies to colonizing cells of other species: E. coli was blocked from invading the interior of *V. cholerae* biofilms unexposed to predation, but they were able to enter biofilms that had been



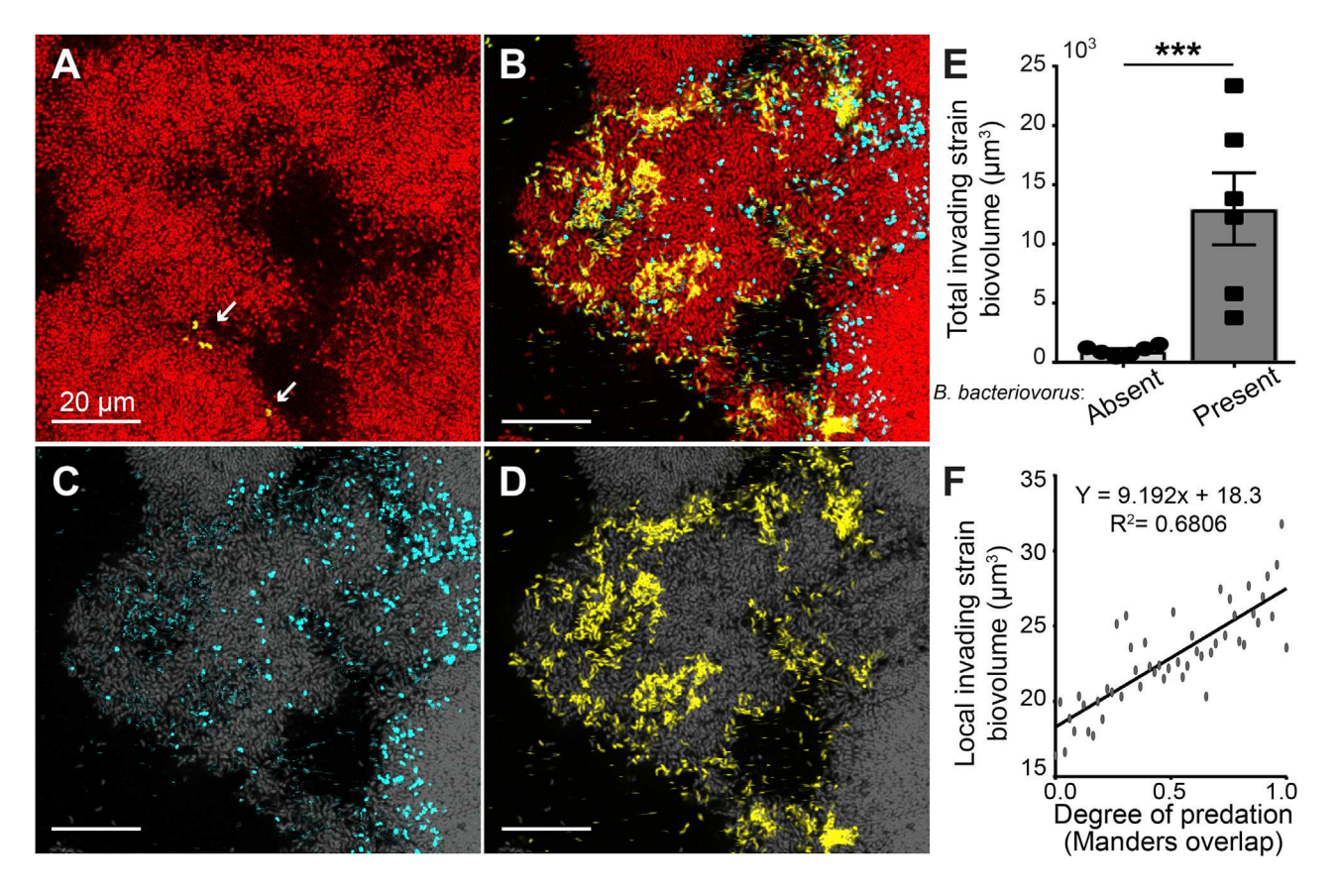


Figure 4. B. bacteriovorus exposure on the periphery of V. cholerae biofilm clusters renders them susceptible to infiltration by other bacteria (A) In the absence of predator exposure, V. cholerae biofilms are highly resistant to invasion by conspecific cells. The resident biofilm is shown in red, and invading cells are shown in vellow.

(B) Resident biofilms that have been exposed to predation by B. bacteriovorus (cyan) have a more loosely structured periphery, and as a result, invading conspecifics are able to enter well past the outer boundary of the resident biofilm.

(C and D) Channel split image from (B) of the predator bacteria (cyan) (C) and channel split image from (B) of invading conspecific cells (yellow) (D) distributed in the outer resident biofilm layers (resident biofilm in gray).

(E) Measurement of the differences in total invading cell biovolume across whole biofilms, in the presence or absence of B. bacteriovorus (***p < 0.001; Wilcoxon signed-rank test with n = 6).

(F) Within biofilms exposed to predation, the degree of invasion by competitors within any given local area scales linearly with the degree of B. bacteriovorus predation in that area.

See also Figure S4.

preyed upon (Figure S4). In this respect, B. bacteriovorus not only alters the structure of the outermost biofilm front but also changes the ecology of biofilm assembly as new and potentially competing (but non-predatory) cells enter the system.

Predator-prey interactions in the context of microbial biofilms are almost certainly widespread in nature; we are only in the early stages of understanding the micrometer-scale processes that determine the outcome of these encounters, the underlying molecular mechanisms of these encounters, and the consequences for microbial ecology and evolution. Major steps forward have recently been made to understand phage-biofilm interaction, $^{32,\overset{'}{5}2,54,55}$ and landmark papers have begun to characterize predation by larger protist predators and cells of metazoan immune systems at high resolution. 46,77-79 B. bacteriovorus, a ubiquitous threat to prey bacteria, has been investigated interacting with biofilms, but primarily via macroscopic assays. 61,63 Here we build on this foundation with the first high-resolution

live imaging and analysis of B. bacteriovorus preying upon biofilms of V. cholerae. The V. cholerae cell-cell packing threshold that we discovered, past which predators are not able to access their prey, reveals novel insights into the mechanisms of biofilm architecture maturation, and it leads to fundamental transformations of biofilm micro-landscape structure and community assembly. These transformations suggest that bacterial predators can act as key modulators of community dynamics, and uncovering how these predators influence more complex biofilms containing multiple prey species is a critical area for future work.

STAR*METHODS

Detailed methods are provided in the online version of this paper and include the following:

• KEY RESOURCES TABLE

Report



- RESOURCE AVAILABILITY
 - Lead Contact
 - Materials availability
 - O Data and code availability
- EXPERIMENTAL MODEL AND SUBJECT DETAILS
- METHOD DETAILS
 - Microfluidic assembly
 - O Biofilm growth conditions and matrix staining
 - Introduction of predators and invading competitor bacteria
 - O Microscopy and image analysis
 - Experimental Design
- QUANTIFICATION AND STATISTICAL ANALYSIS

SUPPLEMENTAL INFORMATION

Supplemental information can be found online at https://doi.org/10.1016/j.cub.2021.03.036.

ACKNOWLEDGMENTS

We thank K.M. Atwood, R.W. Baker, A. Persat, N.W. Rigel, B.D. Ross, D. Schultz, K. Drescher, and members of the Nadell Lab for their comments on the project. We also thank M.A. McPeek for assistance with logistic regression analyses, as well as Dr. Robert Shanks for providing us with the pMQ581 plasmid. B.R.W. is supported by a Gilman Fellowship from the Department of Biological Sciences at Dartmouth. C.D.N. is supported by the Simons Foundation award number 826672, NSF grant MCB 1817342, NSF grant IOS 2017879, a Burke Award from Dartmouth, NIH grant 2R01Al081838 to PI Robert Cramer, NIH grant P20-GM113132 to the Dartmouth BioMT COBRE, and grant RGY0077/2020 from the Human Frontier Science Foundation with co-PI A. Persat.

AUTHOR CONTRIBUTIONS

C.D.N. and D.E.K. conceived the project. C.D.N. supervised the project. C.D.N. and B.R.W. designed experiments. B.R.W. performed experiments and image processing of microscopy data. C.D.N., J.S.A., and B.R.W. analyzed data and produced the figures. D.E.K. and M.E. provided reagents/tools. C.D.N. and B.R.W. wrote the paper with input from D.E.K. C.D.N. acquired funding for the work.

DECLARATION OF INTERESTS

The authors declare that they have no conflicts of interest.

Received: November 17, 2020 Revised: February 2, 2021 Accepted: March 10, 2021 Published: April 6, 2021

REFERENCES

- Duncan, M.C., Gillette, R.K., Maglasang, M.A., Corn, E.A., Tai, A.K., Lazinski, D.W., Shanks, R.M.Q., Kadouri, D.E., and Camilli, A. (2019). High-throughput analysis of gene function in the bacterial predator Bdellovibrio bacteriovorus. MBio 10, e01040-19.
- Rendulic, S., Jagtap, P., Rosinus, A., Eppinger, M., Baar, C., Lanz, C., Keller, H., Lambert, C., Evans, K.J., Goesmann, A., et al. (2004). A predator unmasked: life cycle of Bdellovibrio bacteriovorus from a genomic perspective. Science 303, 689–692.
- Duncan, M.C., Forbes, J.C., Nguyen, Y., Shull, L.M., Gillette, R.K., Lazinski, D.W., Ali, A., Shanks, R.M.Q., Kadouri, D.E., and Camilli, A. (2018). Vibrio cholerae motility exerts drag force to impede attack by the bacterial predator Bdellovibrio bacteriovorus. Nat. Commun. 9, 4757.

- Sockett, R.E. (2009). Predatory lifestyle of Bdellovibrio bacteriovorus. Annu. Rev. Microbiol. 63, 523–539.
- Roschanski, N., Klages, S., Reinhardt, R., Linscheid, M., and Strauch, E. (2011). Identification of genes essential for prey-independent growth of Bdellovibrio bacteriovorus HD100. J. Bacteriol. 193, 1745–1756.
- Kuru, E., Lambert, C., Rittichier, J., Till, R., Ducret, A., Derouaux, A., Gray, J., Biboy, J., Vollmer, W., VanNieuwenhze, M., et al. (2017). Fluorescent Damino-acids reveal bi-cellular cell wall modifications important for Bdellovibrio bacteriovorus predation. Nat. Microbiol. 2, 1648–1657.
- Willis, A.R., Moore, C., Mazon-Moya, M., Krokowski, S., Lambert, C., Till, R., Mostowy, S., and Sockett, R.E. (2016). Injections of predatory bacteria work alongside host immune cells to treat shigella infection in zebrafish larvae. Curr. Biol. 26, 3343–3351.
- Fry, J.C., and Staples, D.G. (1976). Distribution of Bdellovibrio bacteriovorus in sewage works, river water, and sediments. Appl. Environ. Microbiol. 31, 469–474.
- Williams, H.N., Schoeffield, A.J., Guether, D., Kelley, J., Shah, D., and Falkler, W.A., Jr. (1995). Recovery of bdellovibrios from submerged surfaces and other aquatic habitats. Microb. Ecol. 29, 39–48.
- Chauhan, A., and Williams, H.N. (2008). Biostimulation of estuarine microbiota on substrate coated agar slides: a novel approach to study diversity of autochthonous Bdellovibrio- and like organisms. Microb. Ecol. 55, 640–650
- Schoeffield, A.J., and Williams, H.N. (1990). Efficiencies of recovery of bdellovibrios from brackish- water environments by using various bacterial species as prey. Appl. Environ. Microbiol. 56, 230–236.
- 12. Kelley, J.I., and Williams, H.N. (1992). Bdellovibrios in Callinectus sapidus, the blue crab. Appl. Environ. Microbiol. 58, 1408–1410.
- Kelley, J.I., Turng, B., Williams, H.N., and Baer, M.L. (1997). Effects of temperature, salinity, and substrate on the colonization of surfaces in situ by aquatic bdellovibrios. Appl. Environ. Microbiol. 63, 84–90.
- Flemming, H.-C., Wingender, J., Szewzyk, U., Steinberg, P., Rice, S.A., and Kjelleberg, S. (2016). Biofilms: an emergent form of bacterial life. Nat. Rev. Microbiol. 14, 563–575.
- Teschler, J.K., Zamorano-Sánchez, D., Utada, A.S., Warner, C.J.A., Wong, G.C.L., Linington, R.G., and Yildiz, F.H. (2015). Living in the matrix: assembly and control of Vibrio cholerae biofilms. Nat. Rev. Microbiol. 13, 255–268.
- Nadell, C.D., Drescher, K., and Foster, K.R. (2016). Spatial structure, cooperation and competition in biofilms. Nat. Rev. Microbiol. 14, 589–600.
- Datta, M.S., Sliwerska, E., Gore, J., Polz, M.F., and Cordero, O.X. (2016). Microbial interactions lead to rapid micro-scale successions on model marine particles. Nat. Commun. 7, 11965.
- Ebrahimi, A., Schwartzman, J., and Cordero, O.X. (2019). Cooperation and spatial self-organization determine rate and efficiency of particulate organic matter degradation in marine bacteria. Proc. Natl. Acad. Sci. USA 116, 23309–23316.
- Enke, T.N., Leventhal, G.E., Metzger, M., Saavedra, J.T., and Cordero, O.X. (2018). Microscale ecology regulates particulate organic matter turnover in model marine microbial communities. Nat. Commun. 9, 2743.
- Meibom, K.L., Li, X.B.B., Nielsen, A.T., Wu, C.Y., Roseman, S., and Schoolnik, G.K. (2004). The Vibrio cholerae chitin utilization program. Proc. Natl. Acad. Sci. USA 101, 2524–2529.
- Hayes, C.A., Dalia, T.N., and Dalia, A.B. (2017). Systematic genetic dissection of chitin degradation and uptake in Vibrio cholerae. Environ. Microbiol. 19, 4154–4163.
- Wucher, B.R., Bartlett, T.M., Hoyos, M., Papenfort, K., Persat, A., and Nadell, C.D. (2019). Vibrio cholerae filamentation promotes chitin surface attachment at the expense of competition in biofilms. Proc. Natl. Acad. Sci. USA 116, 14216–14221.
- Philippot, L., Raaijmakers, J.M., Lemanceau, P., and van der Putten, W.H. (2013). Going back to the roots: the microbial ecology of the rhizosphere. Nat. Rev. Microbiol. 11, 789–799.

Please cite this article in press as: Wucher et al., Bacterial predation transforms the landscape and community assembly of biofilms, Current Biology (2021), https://doi.org/10.1016/j.cub.2021.03.036



Current Biology Report

- 24. Byrd, A.L., Belkaid, Y., and Segre, J.A. (2018). The human skin microbiome. Nat. Rev. Microbiol. *16*, 143–155.
- 25. Coyte, K.Z., Schluter, J., and Foster, K.R. (2015). The ecology of the microbiome: networks, competition, and stability. Science 350, 663–666.
- Wolcott, R., Costerton, J.W., Raoult, D., and Cutler, S.J. (2013). The polymicrobial nature of biofilm infection. Clin. Microbiol. Infect. 19, 107–112.
- Stacy, A., McNally, L., Darch, S.E., Brown, S.P., and Whiteley, M. (2016).
 The biogeography of polymicrobial infection. Nat. Rev. Microbiol. 14, 93–105
- 28. Hall-Stoodley, L., and Stoodley, P. (2009). Evolving concepts in biofilm infections. Cell. Microbiol. 11, 1034–1043.
- Drescher, K., Dunkel, J., Nadell, C.D., van Teeffelen, S., Grnja, I., Wingreen, N.S., Stone, H.A., and Bassler, B.L. (2016). Architectural transitions in Vibrio cholerae biofilms at single-cell resolution. Proc. Natl. Acad. Sci. USA 113, E2066–E2072.
- Yan, J., Sharo, A.G., Stone, H.A., Wingreen, N.S., and Bassler, B.L. (2016).
 Vibrio cholerae biofilm growth program and architecture revealed by single-cell live imaging. Proc. Natl. Acad. Sci. USA 113, E5337–E5343.
- Drescher, K., Nadell, C.D., Stone, H.A., Wingreen, N.S., and Bassler, B.L. (2014). Solutions to the public goods dilemma in bacterial biofilms. Curr. Biol. 24, 50–55.
- Vidakovic, L., Singh, P.K., Hartmann, R., Nadell, C.D., and Drescher, K. (2018). Dynamic biofilm architecture confers individual and collective mechanisms of viral protection. Nat. Microbiol. 3, 26–31.
- Hibbing, M.E., Fuqua, C., Parsek, M.R., and Peterson, S.B. (2010).
 Bacterial competition: surviving and thriving in the microbial jungle. Nat. Rev. Microbiol. 8, 15–25.
- Martínez-García, R., Nadell, C.D., Hartmann, R., Drescher, K., and Bonachela, J.A. (2018). Cell adhesion and fluid flow jointly initiate genotype spatial distribution in biofilms. PLoS Comput. Biol. 14, e1006094.
- Nadell, C.D., and Bassler, B.L. (2011). A fitness trade-off between local competition and dispersal in Vibrio cholerae biofilms. Proc. Natl. Acad. Sci. USA 108, 14181–14185.
- Schluter, J., Nadell, C.D., Bassler, B.L., and Foster, K.R. (2015). Adhesion as a weapon in microbial competition. ISME J. 9, 139–149.
- Nadell, C.D., Drescher, K., Wingreen, N.S., and Bassler, B.L. (2015).
 Extracellular matrix structure governs invasion resistance in bacterial biofilms. ISME J. 9, 1700–1709.
- 38. Mitri, S., Xavier, J.B., and Foster, K.R. (2011). Social evolution in multispecies biofilms. Proc. Natl. Acad. Sci. USA 108 (Suppl 2), 10839–10846.
- **39.** Nadell, C.D., Xavier, J.B., and Foster, K.R. (2009). The sociobiology of biofilms. FEMS Microbiol. Rev. *33*, 206–224.
- Oliveira, N.M., Martinez-Garcia, E., Xavier, J., Durham, W.M., Kolter, R., Kim, W., and Foster, K.R. (2015). Biofilm formation as a response to ecological competition. PLoS Biol. 13, e1002191.
- Xavier, J.B., and Foster, K.R. (2007). Cooperation and conflict in microbial biofilms. Proc. Natl. Acad. Sci. USA 104, 876–881.
- Coyte, K.Z., Tabuteau, H., Gaffney, E.A., Foster, K.R., and Durham, W.M. (2017). Microbial competition in porous environments can select against rapid biofilm growth. Proc. Natl. Acad. Sci. USA 114, E161–E170.
- Rendueles, O., and Ghigo, J.-M. (2015). Mechanisms of competition in biofilm communities. Microbiol. Spectr. 3, https://doi.org/10.1128/microbiolspec.MB-0009-2014.
- van Gestel, J., Weissing, F.J., Kuipers, O.P., and Kovács, A.T. (2014).
 Density of founder cells affects spatial pattern formation and cooperation in Bacillus subtilis biofilms. ISME J. 8, 2069–2079.
- 45. Dragoš, A., Martin, M., Falcón García, C., Kricks, L., Pausch, P., Heimerl, T., Bálint, B., Maróti, G., Bange, G., López, D., et al. (2018). Collapse of genetic division of labour and evolution of autonomy in pellicle biofilms. Nat. Microbiol. 3, 1451–1460.
- Matz, C., McDougald, D., Moreno, A.M., Yung, P.Y., Yildiz, F.H., and Kjelleberg, S. (2005). Biofilm formation and phenotypic variation enhance

- predation-driven persistence of Vibrio cholerae. Proc. Natl. Acad. Sci. USA 102. 16819–16824.
- 47. Chen, H., and Williams, H.N. (2012). Sharing of prey: coinfection of a bacterium by a virus and a prokaryotic predator. MBio 3, e00051, e12.
- 48. Santos-Lopez, A., Marshall, C.W., Scribner, M.R., Snyder, D.J., and Cooper, V.S. (2019). Evolutionary pathways to antibiotic resistance are dependent upon environmental structure and bacterial lifestyle. eLife 8, e47612.
- Chavez-Dozal, A., Gorman, C., Erken, M., Steinberg, P.D., McDougald, D., and Nishiguchi, M.K. (2013). Predation response of Vibrio fischeri biofilms to bacterivorus protists. Appl. Environ. Microbiol. 79, 553–558.
- Tseng, B.S., Zhang, W., Harrison, J.J., Quach, T.P., Song, J.L., Penterman, J., Singh, P.K., Chopp, D.L., Packman, A.I., and Parsek, M.R. (2013). The extracellular matrix protects Pseudomonas aeruginosa biofilms by limiting the penetration of tobramycin. Environ. Microbiol. 15, 2865–2878.
- Doroshenko, N., Tseng, B.S., Howlin, R.P., Deacon, J., Wharton, J.A., Thurner, P.J., Gilmore, B.F., Parsek, M.R., and Stoodley, P. (2014). Extracellular DNA impedes the transport of vancomycin in Staphylococcus epidermidis biofilms preexposed to subinhibitory concentrations of vancomycin. Antimicrob. Agents Chemother. 58, 7273– 7282.
- Díaz-Pascual, F., Hartmann, R., Lempp, M., Vidakovic, L., Song, B., Jeckel, H., Thormann, K.M., Yildiz, F.H., Dunkel, J., Link, H., et al. (2019). Breakdown of Vibrio cholerae biofilm architecture induced by antibiotics disrupts community barrier function. Nat. Microbiol. 4, 2136–2145.
- Simmons, E.L., Bond, M.C., Koskella, B., Drescher, K., Bucci, V., and Nadell, C.D. (2020). Biofilm structure promotes coexistence of phageresistant and phage-susceptible bacteria. mSystems 5, e00877-19.
- Dunsing, V., Irmscher, T., Barbirz, S., and Chiantia, S. (2019). Purely polysaccharide-based biofilm matrix provides size-selective diffusion barriers for nanoparticles and bacteriophages. Biomacromolecules 20, 3842– 3854.
- Darch, S.E., Kragh, K.N., Abbott, E.A., Bjarnsholt, T., Bull, J.J., and Whiteley, M. (2017). Phage inhibit pathogen dissemination by targeting bacterial migrants in a chronic infection model. MBio 8, e00240-17.
- Wieczorek, A.S., Schmidt, O., Chatzinotas, A., von Bergen, M., Gorissen, A., and Kolb, S. (2019). Ecological functions of agricultural soil bacteria and microeukaryotes in chitin degradation: a case study. Front. Microbiol. 10, 1293.
- Williams, L.E., Cullen, N., DeGiorgis, J.A., Martinez, K.J., Mellone, J., Oser, M., Wang, J., and Zhang, Y. (2019). Variation in genome content and predatory phenotypes between *Bdellovibrio* sp. NC01 isolated from soil and *B. bacteriovorus* type strain HD100. Microbiology (Reading) *165*, 1315–1330
- Li, N., and Williams, H.N. (2015). 454 Pyrosequencing reveals diversity of Bdellovibrio and like organisms in fresh and salt water. Antonie van Leeuwenhoek 107, 305–311.
- 59. de Dios Caballero, J., Vida, R., Cobo, M., Máiz, L., Suárez, L., Galeano, J., Baquero, F., Cantón, R., and Del Campo, R. (2017). Individual patterns of complexity in cystic fibrosis lung microbiota, including predator bacteria, over a 1-year period. MBio 8, e00959-17.
- Shatzkes, K., Tang, C., Singleton, E., Shukla, S., Zuena, M., Gupta, S., Dharani, S., Rinaggio, J., Connell, N.D., and Kadouri, D.E. (2017). Effect of predatory bacteria on the gut bacterial microbiota in rats. Sci. Rep. 7, 43483.
- Kadouri, D., and O'Toole, G.A. (2005). Susceptibility of biofilms to Bdellovibrio bacteriovorus attack. Appl. Environ. Microbiol. 71, 4044– 4051
- Seiler, C., van Velzen, E., Neu, T.R., Gaedke, U., Berendonk, T.U., and Weitere, M. (2017). Grazing resistance of bacterial biofilms: a matter of predators' feeding trait. FEMS Microbiol. Ecol. 93, https://doi.org/10. 1093/femsec/fix112.

Report



- 63. Kadouri, D., Venzon, N.C., and O'Toole, G.A. (2007). Vulnerability of pathogenic biofilms to Micavibrio aeruginosavorus. Appl. Environ. Microbiol.
- 64. Richards, G.P., Fay, J.P., Dickens, K.A., Parent, M.A., Soroka, D.S., and Boyd, E.F. (2012). Predatory bacteria as natural modulators of Vibrio parahaemolyticus and Vibrio vulnificus in seawater and oysters. Appl. Environ. Microbiol. 78, 7455-7466.
- 65. Dashiff, A., Junka, R.A., Libera, M., and Kadouri, D.E. (2011). Predation of human pathogens by the predatory bacteria Micavibrio aeruginosavorus and Bdellovibrio bacteriovorus. J. Appl. Microbiol. 110, 431-444.
- 66. Berk, V., Fong, J.C.N., Dempsey, G.T., Develioglu, O.N., Zhuang, X., Liphardt, J., Yildiz, F.H., and Chu, S. (2012). Molecular architecture and assembly principles of Vibrio cholerae biofilms. Science 337, 236-239.
- 67. Fong, J.C., Rogers, A., Michael, A.K., Parsley, N.C., Cornell, W.-C., Lin, Y.-C., Singh, P.K., Hartmann, R., Drescher, K., Vinogradov, E., et al. (2017). Structural dynamics of RbmA governs plasticity of Vibrio cholerae biofilms. eLife 6, e26163.
- 68. Giglio, K.M., Fong, J.C., Yildiz, F.H., and Sondermann, H. (2013). Structural basis for biofilm formation via the Vibrio cholerae matrix protein RbmA. J. Bacteriol. 195, 3277-3286.
- 69. Hartmann, R., Singh, P.K., Pearce, P., Mok, R., Song, B., Díaz-Pascual, F., Dunkel, J., and Drescher, K. (2019). Emergence of three-dimensional order and structure in growing biofilms. Nat. Phys. 15, 251-256.
- 70. Gallego-Hernandez, A.L., DePas, W.H., Park, J.H., Teschler, J.K., Hartmann, R., Jeckel, H., Drescher, K., Beyhan, S., Newman, D.K., and Yildiz, F.H. (2020). Upregulation of virulence genes promotes Vibrio cholerae biofilm hyperinfectivity. Proc. Natl. Acad. Sci. USA 117, 11010-
- 71. Fong, J.C.N., and Yildiz, F.H. (2007). The rbmBCDEF gene cluster modulates development of rugose colony morphology and biofilm formation in Vibrio cholerae. J. Bacteriol. 189, 2319-2330.
- 72. Beyhan, S., and Yildiz, F.H. (2007). Smooth to rugose phase variation in Vibrio cholerae can be mediated by a single nucleotide change that targets c-di-GMP signalling pathway. Mol. Microbiol. 63, 995–1007.
- 73. Yildiz, F.H., Liu, X.S., Heydorn, A., and Schoolnik, G.K. (2004). Molecular analysis of rugosity in a Vibrio cholerae O1 El Tor phase variant. Mol. Microbiol. 53, 497-515.

- 74. Staver, A.C., and Bond, W.J. (2014). Is there a 'browse trap'? Dynamics of herbivore impacts on trees and grasses in an African savanna. J. Ecol. 102,
- 75. Staver, A.C., Archibald, S., and Levin, S. (2011). Tree cover in sub-Saharan Africa: rainfall and fire constrain forest and savanna as alternative stable states. Ecology 92, 1063-1072.
- 76. Staver, A.C., Archibald, S., and Levin, S.A. (2011). The global extent and determinants of savanna and forest as alternative biome states. Science 334, 230-232,
- 77. Thurlow, L.R., Hanke, M.L., Fritz, T., Angle, A., Aldrich, A., Williams, S.H., Engebretsen, I.L., Bayles, K.W., Horswill, A.R., and Kielian, T. (2011). Staphylococcus aureus biofilms prevent macrophage phagocytosis and attenuate inflammation in vivo. J. Immunol. 186, 6585-6596.
- 78. Van der Henst, C., Scrignari, T., Maclachlan, C., and Blokesch, M. (2016). An intracellular replication niche for Vibrio cholerae in the amoeba Acanthamoeba castellanii. ISME J. 10, 897-910.
- 79. Van der Henst, C., Vanhove, A.S., Drebes Dörr, N.C., Stutzmann, S., Stoudmann, C., Clerc, S., Scrignari, T., Maclachlan, C., Knott, G., and Blokesch, M. (2018). Molecular insights into Vibrio cholerae's intra-amoebal host-pathogen interactions. Nat. Commun. 9, 3460.
- 80. Mukherjee, S., Brothers, K.M., Shanks, R.M.Q., and Kadouri, D.E. (2015). Visualizing Bdellovibrio bacteriovorus by using the tdTomato fluorescent protein. Appl. Environ. Microbiol. 82, 1653-1661.
- 81. Hartmann, R., Jeckel, H., Jelli, E., Singh, P.K., Vaidya, S., Bayer, M., Rode, D.K.H., Vidakovic, L., Díaz-Pascual, F., Fong, J.C.N., et al. (2021). Quantitative image analysis of microbial communities with BiofilmQ. Nat. Microbiol. 6. 151-156.
- 82. Sia, S.K., and Whitesides, G.M. (2003). Microfluidic devices fabricated in poly(dimethylsiloxane) for biological studies. Electrophoresis 24, 3563-
- 83. Weibel, D.B., Diluzio, W.R., and Whitesides, G.M. (2007). Microfabrication meets microbiology. Nat. Rev. Microbiol. 5, 209-218.
- 84. R Development Core Team (2020). R: A Language and Environment for Statistical Computing. Version 4.0.2. http://www.cran.r-project.org/.
- 85. Fox, J., and Weisberg, S. (2019). An R Companion to Applied Regression

Please cite this article in press as: Wucher et al., Bacterial predation transforms the landscape and community assembly of biofilms, Current Biology (2021), https://doi.org/10.1016/j.cub.2021.03.036





STAR***METHODS**

KEY RESOURCES TABLE

REAGENT or RESOURCE	SOURCE	IDENTIFIER
Antibodies		
Cy3 conjugated anti-FLAG	Millipore-Sigma	Cat#A9594
Bacterial Strains and Viruses		
<i>E. coli</i> S17-1 λpir	N/A	Strain S17
E. coli AR 3110, lacZ:Ptac- mKO-κ	N/A	Strain CNE 689
B. bacteriovorus 109J, PMQ581, gfpmut3	This study	Strain 109J
V. cholerae vpvC W240R matrix hyper secretor, lacZ:Ptac-mKate2	This study	Strain CNV 64
V. cholerae N16961 rbmA- 3xFLAG, lacZ:Ptac-mKate2	22	Strain CNV 116
V. cholerae N16961 rbmA- 3xFLAG, lacZ:Ptac-mKO-κ	22	Strain CNV 121
V. cholerae N16961, lacZ:Ptac-mKate2 ∆rbmA	22	Strain CNV 127
V. cholerae vpvC W240R matrix hyper secretor rbmA- 3xFLAG, lacZ:Ptac-mKate2	This study	Strain CNV 252
Chemicals, Peptides, and Recombinant Proteins	S	
Ampicillin	Millipore-Sigma	Cat#A0166
Kanamycin	Millipore-Sigma	Cat#60615
Polymyxin B	Millipore-Sigma	Cat#P4932
MEM Vitamins Solution (100x)	Millipore-Sigma	Cat#M6895
Recombinant DNA		
pBW with N-terminal <i>rbmA</i> -3xFLAG insertion	This study	Plasmid pCN769
pMQ581 Constructed by replacement of tdTomato with gfpmut3 in pMQ414 parental plasmid	80	Plasmid pMQ581
Software and Algorithms		
ZEN Black	Zeiss	Version 2.3
ZEN Blue	Zeiss	Version 2.3
MATLAB	MathWorks	Version R2018b
Paraview	Kitware	Version 5.1.2
Prism	GraphPad	Version 7.02
BiofilmQ	81	Version 0.2.2
R	glm, 'car' package	Version 4.0.2

RESOURCE AVAILABILITY

Lead Contact

More information regarding the resources and reagents used in this study should be directed to the lead contact, Carey Nadell (carey. d.nadell@dartmouth.edu)

Please cite this article in press as: Wucher et al., Bacterial predation transforms the landscape and community assembly of biofilms, Current Biology (2021), https://doi.org/10.1016/j.cub.2021.03.036

Current Biology Report



Materials availability

All plasmids and reagents generated in this study are available upon request to the lead contact, Carey Nadell.

Data and code availability

All raw data generated for this paper are available upon request to the lead contact, Carey Nadell.

EXPERIMENTAL MODEL AND SUBJECT DETAILS

Prior to experiments, V. cholerae and E. coli strains were grown overnight in lysogeny broth medium (LB) in a shaking incubator at 37° C. B. bacteriovorus were obtained via co-culture using E. coli WM 3064 as prey; these co-cultures were incubated at 30° C for 24 h, and predators were purified by filtration using 0.45° m Millex pore-size filter (Millipore, Billerica, MA, USA) in order to remove any remaining prey debris. B. bacteriovorus was washed by centrifugation (13,000 rpm for 45° min) and resuspended in fresh buffer to reach a final concentration of $\sim 5 \times 10^9$ PFU/mL. B. bacteriovorus cultivation and isolation protocols have been described in additional detail previously. Standard molecular cloning techniques were used to construct the strains used in this study. Modifications to V. cholerae were made using E. coli strain S-17- λ pir carrying the allelic exchange vector pBW1 as previously described. Antibiotics and reagents used for counter selection were used at the following concentrations: $100 \mu g/mL$ ampicillin, $50 \mu g/mL$ kanamycin, $50 \mu g/mL$ polymyxin B, 5% sucrose. All reagents were obtained from Millipore Sigma unless otherwise stated. All biofilm experiments were performed in M9 minimal medium, with the addition of 2 mM MgSO₄, $100 \mu g/mL$ MEM vitamins, 0.5% glucose, and $15 \mu g/mL$ thanolamine (pH 7.1).

METHOD DETAILS

Microfluidic assembly

Poly-dimethylsiloxane (PDMS) was used to cast microfluidic chambers using standard soft lithography techniques. ^{82,83} The chambers were bonded to #1.5 coverslips measuring 36mm by 60 mm (WxL). The chambers used for this study had dimensions of 3000μm x 500μm x 75μm (LxWxD). In order to run media through these chambers, 1mL of M9 with 0.5% glucose was loaded into 1mL BD plastic syringes. 25-gauge needles were affixed to the syringes and #30 Cole Palmer PTFE tubing with an inner diameter of 0.3mm was placed over the end of the needle. The other end of this tubing was then placed into pre-bored holes in the microfluidic devices. An additional length of tubing was run from the auxiliary channels in the device to a vacuum line, which prevented bubbles from entering the system. Syringes were mounted to Pico Plus Syringe Pumps (Harvard Apparatus)

Biofilm growth conditions and matrix staining

Biofilms were grown in microfluidic chambers that were fabricated as described above. Overnight cultures of V. cholerae were backdiluted into M9 minimal medium with 0.5% glucose and allowed to re-enter exponential phase ($OD_{600} = 1.0$) to acclimate to the media conditions used for biofilm growth (M9 minimal media with 0.5% glucose). These cultures were inoculated into chambers without flow to allow surface colonization for 1 h. After this period, a flow rate of $0.2\mu L/min$ was established for the remainder of the experiment. All experiments were performed at room temperature. For matrix staining experiments in which V. cholerae harbored an N-terminal fusion of 3xFLAG to RbmA, a monoclonal anti-FLAG antibody conjugated to a Cy3 fluorophore added to the influx medium at $1\mu g/mL$.

Introduction of predators and invading competitor bacteria

Introduction of predators was performed in a similar fashion to the method used for initial chamber inoculation with V. cholerae. B. bacteriovorus ($OD_{600} = 1.0$; $\sim 2.5 \times 10^9$ PFU/mL) was inoculated into the system by gently removing the sterile media inlet tubing and introducing $20 \mu L$ of B. bacteriovorus chambers via micropipette. The media tubing was then returned to its position, and flow was resumed 30 min after introduction of predators. For experiments in which biofilms were challenged with either invading V. cholerae or E. coli, a similar regime was carried out. Overnight cultures of V. cholerae or E. coli housing a different fluorescent protein than the resident biofilms were diluted to an OD600 of 1.0 and then inoculated into the chambers. Tubing was replaced and flow was resumed 30 min after introduction of the invading strain.

Microscopy and image analysis

Imaging of the biofilms was performed with a Zeiss LSM 880 laser scanning confocal microscope, fitted with a 40x /1.2 N.A. water objective or a 10x/ 0.4 N.A. water objective. A 488-nm laser line was used to excite the GFP produced constitutively by *B. bacteriovorus*. To Image *V. cholerae*, a 594-nm laser was used to excite mKate2 in the resident strain, and a 543-nm laser was used to excite mKO-κ for the invading strain. For experiments in which RbmA matrix was imaged, the 543-nm laser was used to excite the Cy-3 fluorophore conjugated to the anti-FLAG antibody used for RbmA immunostaining. Microscope hardware was controlled by the native Zeiss Zen Black software. To obtain data for image analysis, several image stacks were taken at independent locations within different chamber replicates. These image stacks were then analyzed using the BiofilmQ framework. A detailed explanation of BiofilmQ is developed in a dedicated publication.⁸¹ 3D renderings were created by first using the VTK output feature present in BiofilmQ. These files could then be processed in ParaView and rendered using Osprey ray tracing.

Please cite this article in press as: Wucher et al., Bacterial predation transforms the landscape and community assembly of biofilms, Current Biology (2021), https://doi.org/10.1016/j.cub.2021.03.036





Experimental Design

All experiments were carried out with n independent biological replicas, with sample sizes for each experiment noted in the respective figure legends; all data were processed and analyzed using the BiofilmQ framework as noted above. In each replicate, the number of individual bacteria is variable, as biofilm size can vary between chambers. Blinding of these replicates does not apply, and no data were excluded from the study.

QUANTIFICATION AND STATISTICAL ANALYSIS

Logistic regression (generalized linear models with binomial errors in R version 4.0.284) was used to analyze data in Figure 2 to assess how local matrix accumulation, local biovolume fraction, and neighborhood biovolume fraction contributed to the probability of predation for WT and matrix hyper-secreting biofilms of V. cholerae (see Tables S1 and S2 with accompanying discussion). For these analyses, the degree of overlap between B. bacterivorous and V. cholerae in each unit of the 3-D grid was transformed into a binary variable, with 0 indicating no overlap (predation absent) and 1 indicating some overlap (predation present). Variance inflation factors were calculated to test for problematic collinearity among predictors, 85 of which none was found. Kolmogorov-Smirnov tests were used for comparisons of frequency distributions in the Supplemental Information. Wilcoxon signed ranks tests were used for pairwise comparisons of microcolony area in different biofilm landscapes in Figure 3, as well as the differences in the biovolume of invading individuals in Figure 4. For all datasets, sample sizes are stated in each corresponding figure legend.